Liquid-liquid phase separation in particles containing secondary organic material free of inorganic salts

Mijung Song[1,2], Pengfei Liu[3], Scot T. Martin[3,4], Allan K. Bertram[2*]

[1] {Department of Earth and Environmental Sciences, Chonbuk National University, Jeollabuk-do, Republic of Korea}

[2] {Department of Chemistry, University of British Columbia, Vancouver, BC, V6T 1Z1, Canada}

[3] {John A. Paulson School of Engineering and Applied Sciences, Harvard University, Cambridge, Massachusetts 02138, USA}

[4] {Department of Earth and Planetary Sciences, Harvard University, Cambridge, Massachusetts 02138, USA}

Correspondence to: A. K. Bertram (bertram@chem.ubc.ca)

Abstract

Particles containing secondary organic material (SOM) are ubiquitous in the atmosphere and play a role in climate and air quality. Recently, research has shown that liquid-liquid phase separation (LLPS) occurs at high relative humidities (RH) (greater than ~ 95 %) in α-pinene-derived SOM particles free of inorganic salts while LLPS does not occur in isoprene-derived SOM particles free of inorganic salts. We expand on these findings by investigating LLPS at 290 ± 1 K in SOM particles free of inorganic salts produced from ozonolysis of β-caryophyllene, ozonolysis of limonene, and photo-oxidation of toluene. LLPS was observed at greater than ~95 % RH in the biogenic SOM particles derived from β-caryophyllene and limonene while LLPS was not observed in the anthropogenic SOM particles derived from toluene. This work combined with the earlier work on LLPS in SOM particles free of inorganic salts suggests that the occurrence of LLPS in SOM particles free of inorganic salts is related to the oxygen-to-carbon elemental ratio (O:C) of the organic material. These results help explain the difference between the hygroscopic parameter

κ of SOM particles measured above and below water saturation in the laboratory and field, and have implications for predicting the cloud condensation nucleation properties of SOM particles.

1 Introduction

Secondary organic material (SOM) is produced in the atmosphere by the oxidation of volatile organic compounds (VOCs) such as α-pinene and isoprene from trees and toluene from anthropogenic sources. Once formed, the low volatility and semivolatile oxidation products can partition to the particle phase to form SOM containing particles (Hallquist et al., 2009; Ervens et al., 2011). SOM accounts for approximately 20 – 80 % of the submicrometer particle mass in the atmosphere (Zhang et al., 2007; Jimenez et al., 2009). Although the exact chemical composition of SOM in atmospheric particles remains an active area of research, laboratory and field studies have shown that the average oxygen-to-carbon elemental ratio (O:C) of these particles ranges from 0.2 to 1.0 (Chen et al., 2009; Jimenez et al., 2009; Heald et al., 2010; Takahama et al., 2011).

As the relative humidity (RH) varies in the atmosphere, SOM containing particles can undergo several different phase transitions with implications for the cloud condensation nuclei (CCN) properties, optical properties, reactivity, and growth of these particles (Martin et al., 2000; Raymond and Pandis, 2002; Bilde and Svenningsson, 2004; Zuend et al., 2010; Kuwata and Martin, 2012; Brunamonti et al., 2015). One possible phase transition that SOM particles may undergo as RH varies in the atmosphere is liquid-liquid phase separation (LLPS) (Pankow, 2003; Marcolli et al., 2006; Ciobanu et al., 2009: Zuend and Seinfeld, 2012; Veghte et al., 2013; O'Brien et al., 2015). LLPS in particles containing both SOM and inorganic salts has been the focus of many recent studies. These studies have shown that SOM particles mixed with inorganic salts can undergo LLPS in the atmosphere when the O:C of the organic material is less than 0.56, but LLPS may not occur when the O:C of the organic material is greater than 0.80 (Bertram et al., 2011; Krieger et al., 2012; Smith et al., 2012; Song et al., 2012a; Schill and Tolbert, 2013; Song et al., 2013; You et al., 2013; You et al., 2014).

Recently, researchers have also focused on LLPS in SOM particles free of inorganic salts. Petters et al. (2006) suggested that a miscibility gap in particles containing organic polymers at high RH may lead to a non-classical pathway for CCN activation. Renbaum-Wolff et al. (2016) showed that α-pinene-derived SOM free of inorganic salts can undergo LLPS at high RH values (~95 to 100 %),

which could result in altered CCN properties. In addition, they showed that LLPS in SOM particles will lead to a different hygroscopic parameter, κ, at subsaturated conditions compared to supersaturated conditions. The implication is that the CCN activity of SOM particles, if they undergo LLPS, is higher than predicted from subsaturated hygroscopicity measurements. Related, Hodas et al. (2016), using a combination of measurements and modelling of surrogates of oligomers, showed that the prevalence of LLPS at high RH can contribute to differences in hygroscopicity above and below water saturation. Most recently, Rastak et al. (2017) observed that isoprene-derived SOM particles do not undergo LLPS even at high RH. Rastak et al. (2017) used these results together with thermodynamic calculations to explain the hygroscopic properties of biogenic organic aerosol particles in the laboratory and the field.

Here we expand on the studies by Renbaum-Wolff et al. (2016) and Rastak et al. (2017) by investigated LLPS in SOM particles generated by the ozonolysis of limonene, ozonolysis of β-caryophyllene, and photo-oxidation of toluene. Limonene and β-caryophyllene are both biogenic VOCs, while toluene is an anthropogenic VOC (Kanakidou et al., 2005). Both limonene-derived and β-caryophyllene-derived SOM particles have been used as proxies of biogenic SOM particles in the atmosphere (Bateman et al., 2009; Alfarra et al., 2012; Kundu et al., 2012; Frosch et al., 2013; Liu et al., 2013), while toluene-derived SOM has been used as a proxy for anthropogenic SOM particles (Pandis et al., 1992; Robinson et al., 2013; Liu et al., 2016; Song et al., 2016; Ye et al., 2016).

2 Methods

2.1 Production of secondary organic materials

SOM particles were generated via β-caryophyllene ozonolysis and limonene ozonolysis in a flow tube reactor (Table 1) and via toluene photo-oxidation in an oxidation flow reactor (OFR) (Table 2). The method of particle generation in the flow tube reactor was described in Shrestha et al. (2013) and the methods of particle generation in the OFR (Kang et al., 2007) were given in Liu et al. (2015). The flow tube reactor was operated at a flow rate of 3.5 L min^{-1} (with a residence time of 38 s) and < 5% RH. The OFR was operated at flow rates of 7.0 to 9.5 L min^{-1} (with a residence time of 80 to 110 s) and 13 ± 3 % RH. Both reactors were operated at a temperature of 293 ± 2 K.

Table 1 lists the experimental conditions for the production of SOM via ozonolysis. For the particle generation via ozonolysis, ozone was produced by irradiating pure air (Aadco 737 Pure Air Generator) with ultraviolet emission from a mercury lamp (λ = 185 nm). Ozone concentrations used for ozonolysis ranged from 12 - 30 ppm for β-caryophyllene and 13 - 30 ppm for limonene (Table 1). β-caryophyllene and limonene (Sigma Aldrich, ≥ 99 %) were dissolved in 2-butanol (Sigma-Aldrich, ≥ 99.5 %). These organic solutions were injected into a glass round-bottom flask held at 310 K, where the organic liquids vaporized at the tip of a syringe. The organic vapor was then swept into the reactor where ozonolysis took place to form SOM and particles. The injected precursor concentrations were 0.03 - 0.7 ppm for β-caryophyllene and 0.07 - 2.0 ppm for limonene in the main flow of the reactor. In the ozonolysis experiments, butanol served as an OH radical scavenger.

Table 2 presents the experimental conditions for the production of SOM via photo-oxidation. For the particle generation via photo-oxidation, hydroxyl radicals were produced in the OFR by the photochemical reactions:

$$O_3 + h\nu \rightarrow O_2 + O(^1D), \quad \text{(R1)}$$

$$O(^1D) + H_2O \rightarrow 2OH \quad \text{(R2)}$$

Ozone was again produced by irradiating pure air (Aadco 737 Pure Air Generator) with ultraviolet emission from a mercury lamp (λ = 185 nm). Ozone concentrations used in the photo-oxidation studies were 30 ppm (Table 2). Toluene (Sigma-Aldrich, 99 %) was injected and vaporized in a flask, and the vapors were swept into the OFR by purified air. The injected toluene concentrations were 0.2 - 1.0 ppm.

The mass concentration of SOM particles during the generation process was determined from measurements of the number-diameter distribution of SOM particles in the flow tube reactor or OFR and assuming a material density of 1200 kg m^{-3} (Liu et al., 2013). The number-diameter distributions were measured with a scanning mobility particle sizer (SMPS; TSI Inc.). The O:C ratio of the toluene-derived SOM studied here was determined using a high resolution aerosol mass

spectrometer (HR-ToF-AMS; Aerodyne Research Inc.). Data analysis was based on the approach described by Chen et al. (2011).

2.2 Production of supermicron SOM particles on hydrophobic substrates

At the outlet of the flow tube reactor and OFR, the sub-micrometer SOM particles were collected on hydrophobic surfaces. The limonene-derived SOM and toluene-derived SOM particles were collected onto glass slides coated with trichloro(*1H,1H,2H,2H*-perfluorooctyl)silane (Sigma-Aldrich, 97%). The coating procedure is described in Knopf (2003). The β-caryophyllene-derived SOM particles were collected onto Teflon substrates.

Two different methods were used to collect submicron particles on hydrophobic substrates (see Tables 1 and 2). The first method used was an electrostatic precipitator (TSI 3089, USA). In this case, the resulting SOM particles on the hydrophobic substrates were smaller than ~10 µm. From experience in our laboratory, detection of LLPS with our microscope setup is the clearest when the size of the particles are roughly 20 - 80 µm. As a result, the following method was used to coagulate the sub-10 µm particles into 20 - 80 µm particles: first the substrate containing the SOM particles was placed in a RH-controlled flow-cell (Parsons et al., 2004; Pant et al., 2006; Song et al., 2012b). The RH in the flow-cell was then set to over 100 % for 30 - 60 min to grow and coagulate the SOM particles. The RH in the flow-cell was then decreased to ~80 - 90 % RH to evaporate the water. During the experiments, the particles were observed using a reflectance microscope (Zeiss Axiotech, 50×). These growth and coagulation processes resulted in SOM particles consisting of 20 - 80 µm in diameter (Song et al., 2015; Renbaum-Wolff et al., 2016).
In the second method used to collect SOM particles collected on a hydrophobic substrate, a single stage impactor was used (Prenni et al., 2009; Pöschl et al., 2010; Hosny et al., 2016). In this case, the SOM particles after collection were as big as 100 µm due to coagulation during the collection process. Since the particles were already large enough for the LLPS experiments, they were used directly without the need for the growth and coagulation experiments described above. Both methods used to collect SOM particles collected both the water-soluble and water-insoluble components of the SOM particles.

2.3 Optical microscopy of supermicron SOM particles

For the LLPS experiments, the hydrophobic substrate containing SOM particles with sizes in the range of 20 to 80 μm in diameters was mounted in a temperature and RH controlled flow-cell coupled to an optical reflectance microscope (Zess Axiotech, 50× objective) (Parsons et al., 2004; Pant et al., 2006; Song et al., 2012b). The temperature of the cell was 290 ± 1 K in all experiments. RH in the cell was regulated by varying the ratio of a dry and humidified N_2 flow. The total flow rate was ~1200 sccm. The RH was determined from measurements of the temperature with a thermocouple and measurements of the dew point/frost point with a chilled mirror sensor (General Eastern, Canada). The RH was calibrated using the deliquescence RH for pure ammonium sulfate particles (80% RH at 293 K, Martin, 2000). After calibration, the uncertainty of the RH was ± 2.0 % based on the reproducibility of multiple deliquesce measurements. At the beginning of LLPS experiments the SOM particles were equilibrated at ~100 % RH for 15 minutes. Then the RH was reduced from ~100 to ~0 % RH at a rate of 0.1 to 0.5 % RH min^{-1}, and subsequently increased to ~100 % RH at a rate of 0.1 to 0.5 % RH min^{-1}. We did not observe a dependence of LLPS on the RH ramp rate, although only a narrow range of rates were used. During the humidity cycle, optical images of the SOM particles were recorded every 5 - 10 seconds using a CCD camera.

3 Results and Discussion

3.1 β-caryophyllene-derived and limonene-derived SOM particles

Humidity cycles at 290 ± 1 K were performed for β-caryophyllene-derived SOM particles generated with mass concentrations of 15 - 4000 μg m^{-3} and limonene-derived SOM generated with mass concentrations of 80 - 7000 μg m^{-3} (Table 1). In all cases, LLPS was observed at high RH. Table 1 summarizes the results during humidity cycles. Shown in Fig. 1a and Movie S1 (Supplementary Material) are examples of optical images of a β-caryophyllene-derived SOM particle as a function of increasing RH for the particle mass concentrations of 2000 - 4000 μg m^{-3}. Shown in Fig. 1b and Movie S2 (Supplementary Material) are examples of optical images of a limonene-derived SOM particle as a function of increasing RH for the particle mass concentrations of 7000 μg m^{-3}. For both types of SOM particles, only one phase was observed for RH values from 0 to ~ 90 %. Note, the light-colored circle in the center of the particles at 90.5 % RH for β-

caryophyllene-derived SOM and at 95.0 % RH for limonene-derived SOM is an optical effect due to the light scattering from a hemispherical particle (Bertram et al., 2011). In Fig. 1, LLPS is observed at 91.5 % RH for the β-caryophyllene-derived SOM particle and at 95.3 % RH for the limonene-derived SOM particle. LLPS began with the formation of many small inclusions of a second phase, and in both cases the phase transition occurred over a narrow range of RH. The small inclusions coagulated to larger droplets in the β-caryophyllene-derived SOM at 92.5 % RH and in the limonene-derived SOM at 96.1 % RH (Figs. 1a and 1b). At the highest RH investigated, a core-shell shell morphology is observed. Such a core-shell morphology on a hydrophobic substrate has been observed previously in organic/ammonium sulfate/H_2O particles by Song et al. (2012b), although a different morphology can result in the absence of the hydrophobic substrate (Reid et al., 2011). After formation of the core-shell morphology consisting of an inner and outer phase, the two liquid phases co-existed as high as ~100 % RH. We assume that the inner phase is a water-rich phase while the other phase is an organic-rich phase, since the size of the inner phase decreases as the RH decreases (Renbaum-Wolff et al., 2016). The surface tension of water and the surface tension of more-oxidized and less oxidized organics is consistent with this assumption (Jasper, 1972). Upon drying, the two liquid phases merge into one liquid phase. This mixing process occurred at 90.9 % RH for β-caryophyllene-derived SOM and 95.6 % RH for limonene-derived SOM. Movies of the mixing process are shown in the Supplementary Material (Movies S3 and S4).

Shilling et al. (2009) showed that the O:C of SOM can depend on the particle mass concentration used to generate the SOM. To determine whether the occurrence of LLPS depends on the SOM particle mass concentrations used when generating the SOM, particle mass concentrations ranging from 15 – 7000 μg m^{-3} were investigated (Table 1). Illustrated in Fig. 2a and 2b is the RH at which two phases were observed during humidity cycles as a function of the mass concentrations of the β-caryophyllene-derived and limonene-derived SOM samples. Triangles represent mixing relative humidites (MRH) of two liquid phases upon drying and circles represents separation relative humidity (SRH) upon moistening.

LLPS was observed at 93.6 ± 1.5 % RH in the β-caryophyllene-derived SOM particles for the particle mass concentrations of 15 – 4000 μg m^{-3} (Fig. 2a). In the limonene-derived SOM particles, LLPS occured at 96.1 ± 2.1 % RH for the particle mass concentrations of 80 – 7000 μg m^{-3} (Fig.

2b). LLPS occurred at 96.0 ± 0.7 % RH in α-pinene-derived SOM particles for the mass concentrations of 75 - 11000 µg m^{-3} (Renbaum-Wolff et al., 2016) (Fig. 2c). As shown in Fig. 2, the SRH and MRH of the β-caryophyllene-derived SOM, limonene-derived SOM, and α-pinene-derived SOM particles do not depend strongly on the SOM particle mass concentrations used to generate the SOM.

3.2 Toluene-derived SOM

Humidity cycles were also performed for SOM particles generated from photo-oxidation of toluene using particle mass concentrations of 80 - 1000 µg m^{-3} in the reactor (Table 2). None of the toluene-derived SOM particles underwent LLPS during RH cycling even at high RH (Table 2).

Shown in Fig. 3 and Movie S5 (Supplementary Material) are optical images of a toluene-derived SOM particle for mass concentrations of 80 - 100 µg m^{-3}. Images in Fig. 3 and Movie S5 were recorded as the RH was increased. No LLPS was observed in the SOM particle during RH cycling between 0 and 100 %. Rastak et al. (2017) did not observe LLPS in isoprene-derived SOM particles for the mass concentrations of 60 - 1000 µg m^{-3}

3.3 Relation between LLPS and O:C.

Summarized in Table 3 are the average SRH and MRH values determined in our work and by Renbaum-Wolff et al. (2016) and Rastak et al. (2017). The average SRH and MRH values are based on several cycles of RH for different SOM mass concentrations. Also included in Table 3 are the average O:C values for the studied SOM particles. The average O:C values for SOM from toluene photo-oxidation are based on the current study (Section 2.1). The average O:C values for the other SOM are taken from the literature. Since the average O:C can depend on oxidant time and oxidation conditions, we chose literature data that were closest to the experimental conditions used when studying LLPS (Supplementary Material, Section S1 and Table S1).

Based on the data shown in Table 3, there appears to be a relationship between the occurrence of LLPS and the average O:C of the organic material: when the average O:C was between 0.34 and 0.44, LLPS was observed, but when the average O:C was between 0.52 and 1.30, LLPS was not

observed. This trend is also apparent in Fig. 4a, where SRH data in Table 3 is plotted versus the O:C data in Table 3.

SOM have an average O:C and a spread (or distribution) of O:C values. Similar to SOM, systems containing two organics and water also have a spread in O:C and an average O:C. Hence, as a starting point to understanding LLPS in SOM, we considered previous studies that explored the miscibility gap in bulk solutions containing two organics and water (see Table 1 in Ganbavale et al., 2015). When the average O:C of the organic material was low in a system containing two organic components with water, LLPS was observed. For example, LLPS was observed in a mixture of 1-butanol (O:C = 0.25), 1-propanol (O:C = 0.20), and water (Gomis-Yagües et al., 1998) and in a mixture of 1-pentanol (O:C = 0.20), acetone (O:C=0.33), and water (Tiryaki et al., 1994). On the other hand, when the average O:C of the organic material was high in a system containing two organics and water, LLPS was not observed. For example, LLPS was not observed in a mixture of acetic acid (O:C=1.00), ethanol (O:C=0.50), and water (Pickering, 1893). We conclude that the relationship between average O:C and LLPS in SOM observed here is not inconsistent with previous LLPS studies in systems containing two organics and water. In addition to the average O:C, the spread in O:C in organic mixtures will also be important for LLPS (Renbaum-Wolff et al., 2016).

4. Implications

As mentioned in the introduction, Petters et al. (2006), Hodas et al. (2016), Renbaum-Wolff et al. (2016), and Rastak et al. (2017) showed using thermodynamic calculations that SOM particles that undergo LLPS at high RH values have modified CCN properties. Hence, LLPS should be considered when predicting the CCN properties of SOM particles derived from α-pinene ozonolysis, β-caryophyllene ozonolysis, and limonene ozonolysis. A caveat is that the mass concentrations used when generating the SOM particles in our experiments was larger than normally found in the atmosphere (Zhang et al., 2007; Jimenez et al., 2009; Spracklen et al., 2011; Li et al., 2015). Additional studies are needed to confirm LLPS in SOM particles generated using more atmospherically relavant SOM mass concentrations.

Discrepancy between the hygroscopic parameter, κ, (Petters and Kreidenweis, 2007) measured below water saturation (κ_{HGF}) and above water saturation (κ_{CCN}) in SOM particles have been reported in several studies (Petters et al., 2006; Prenni et al., 2007; Juranyi et al., 2009; Petters et al., 2009; Good et al., 2010; Irwin et al., 2010; Massoli et al., 2010; Dusek et al., 2011; Irwin et al., 2011; Hersey et al., 2013; Pajunoja et al., 2015; Zhao et al., 2016). Petters et al. (2006), Hodas et al. (2016), Renbaum-Wolff et al. (2016) and Rastak et al. (2017) suggested that such discrepancies are expected in systems that undergo LLPS at high RH. Summarized in Table 4 and Fig. 4b is literature data on the difference between κ_{HGF} and κ_{CCN} (denoted $\Delta\kappa$) as a function of average O:C of the organic material studied (Prenni et al., 2007; Massoli et al., 2010; Pajunoja et al., 2015). The experimental conditions (oxidation time and oxidation level) for the studies reported in Table 4 were not necessarily similar to the experimental conditions for the studies reported in Table 3, even if the same precursor volatile organic compound was used.

Figure 4b suggests that $\Delta\kappa$ is related to the average O:C of the organic material. Figure 4a and 4b combined suggests that when the average O:C is small, LLPS occurs and the difference between κ_{HGF} and κ_{CCN} is large. On the other hand, when the average O:C is large, LLPS does not occur and the difference between κ_{HGF} and κ_{CCN} is small. Figure 4 provides additional support for the suggestion that the LLPS is related to the discrepancies between κ_{HGF} and κ_{CCN}.

Acknowledgments

This work was supported by the Natural Sciences and Engineering Research Council of Canada. Support from the US National Science Foundation (AGS-1640378) and the US Department of Energy (DE-SC0012792) is also acknowledged. Mijung Song acknowledges support from a National Research Foundation of Korea (NRF) grant funded by the Korea Government (MSIP) (2016R1C1B1009243).

References

Aiken, A. C., Decarlo, P. F., Kroll, J. H., Worsnop, D. R., Huffman, J. A., Docherty, K. S., Ulbrich, I. M., Mohr, C., Kimmel, J. R., Sueper, D., Sun, Y., Zhang, Q., Trimborn, A., Northway, M.,

Ziemann, P. J., Canagaratna, M. R., Onasch, T. B., Alfarra, M. R., Prevot, A. S. H., Dommen, J., Duplissy, J., Metzger, A., Baltensperger, U., and Jimenez, J. L.: O/C and OM/OC ratios of primary, secondary, and ambient organic aerosols with high-resolution time-of-flight aerosol mass spectrometry, Environ. Sci. Technol., 42, 4478-4485, Doi 10.1021/Es703009q, 2008.

Alfarra, M. R., Hamilton, J. F., Wyche, K. P., Good, N., Ward, M. W., Carr, T., Barley, M. H., Monks, P. S., Jenkin, M. E., Lewis, A. C., and McFiggans, G. B.: The effect of photochemical ageing and initial precursor concentration on the composition and hygroscopic properties of beta-caryophyllene secondary organic aerosol, Atmos. Chem. Phys., 12, 6417-6436, 10.5194/acp-12-6417-2012, 2012.

Bateman, A. P., Nizkorodov, S. A., Laskin, J., and Laskin, A.: Time-resolved molecular characterization of limonene/ozone aerosol using high-resolution electrospray ionization mass spectrometry, Phys. Chem. Chem. Phys., 11, 7931-7942, 10.1039/b905288g, 2009.

Bertram, A. K., Martin, S. T., Hanna, S. J., Smith, M. L., Bodsworth, A., Chen, Q., Kuwata, M., Liu, A., You, Y., and Zorn, S. R.: Predicting the relative humidities of liquid-liquid phase separation, efflorescence, and deliquescence of mixed particles of ammonium sulfate, organic material, and water using the organic-to-sulfate mass ratio of the particle and the oxygen-to-carbon elemental ratio of the organic component, Atmos. Chem. Phys., 11, 10995-11006, Doi 10.5194/acp-11-10995-2011, 2011.

Bilde, M., and Svenningsson, B.: CCN activation of slightly soluble organics: the importance of small amounts of inorganic salt and particle phase, Tellus B, 56, 128-134, Doi 10.1111/j.1600-0889.2004.00090.x, 2004.

Brunamonti, S., Krieger, U. K., Marcolli, C., and Peter, T.: Redistribution of black carbon in aerosol particles undergoing liquid-liquid phase separation, Geophys. Res. Lett., 42, 2532-2539, Doi 10.1002/2014gl062908, 2015.

Chen, Q., Farmer, D. K., Schneider, J., Zorn, S. R., Heald, C. L., Karl, T. G., Guenther, A., Allan, J. D., Robinson, N., Coe, H., Kimmel, J. R., Pauliquevis, T., Borrmann, S., Poschl, U., Andreae, M. O., Artaxo, P., Jimenez, J. L., and Martin, S. T.: Mass spectral characterization

of submicron biogenic organic particles in the Amazon Basin, Geophys. Res. Lett., 36, Artn L2080610.1029/2009gl039880, 2009.

Chen, Q., Liu, Y. J., Donahue, N. M., Shilling, J. E., and Martin, S. T.: Particle-Phase Chemistry of Secondary Organic Material: Modeled Compared to Measured O:C and H:C Elemental Ratios Provide Constraints, Environ. Sci. Technol., 45, 4763-4770, 10.1021/es104398s, 2011.

Chhabra, P. S., Ng, N. L., Canagaratna, M. R., Corrigan, A. L., Russell, L. M., Worsnop, D. R., Flagan, R. C., and Seinfeld, J. H.: Elemental composition and oxidation of chamber organic aerosol, Atmos. Chem. Phys., 11, 8827-8845, 10.5194/acp-11-8827-2011, 2011.

Ciobanu, V. G., Marcolli, C., Krieger, U. K., Weers, U., and Peter, T.: Liquid-Liquid Phase Separation in Mixed Organic/Inorganic Aerosol Particles, J. Phys. Chem. A., 113, 10966-10978, Doi 10.1021/Jp905054d, 2009.

Dusek, U., Frank, G. P., Massling, A., Zeromskiene, K., Iinuma, Y., Schmid, O., Helas, G., Hennig, T., Wiedensohler, A., and Andreae, M. O.: Water uptake by biomass burning aerosol at sub- and supersaturated conditions: closure studies and implications for the role of organics, Atmos. Chem. Phys., 11, 9519-9532, 10.5194/acp-11-9519-2011, 2011.

Ervens, B., Turpin, B. J., and Weber, R. J.: Secondary organic aerosol formation in cloud droplets and aqueous particles (aqSOA): a review of laboratory, field and model studies, Atmos. Chem. Phys., 11, 11069-11102, DOI 10.5194/acp-11-11069-2011, 2011.

Frosch, M., Bilde, M., Nenes, A., Praplan, A. P., Juranyi, Z., Dommen, J., Gysel, M., Weingartner, E., and Baltensperger, U.: CCN activity and volatility of beta-caryophyllene secondary organic aerosol, Atmos. Chem. Phys., 13, 2283-2297, 10.5194/acp-13-2283-2013, 2013.

Ganbavale, G., Zuend, A., Marcolli, C., and Peter, T.: Improved AIOMFAC model parameterisation of the temperature dependence of activity coefficients for aqueous organic mixtures, Atmos. Chem. Phys., 15, 447-493, 10.5194/acp-15-447-2015, 2015.

Gomis-Yagues, V., Ruiz-Bevia, F., Ramos-Nofuentes, M., and Fernandez-Torres, M. J.: The influence of the temperature on the liquid-liquid equilibrium of the ternary system 1-butanol-1-propanol-water, Fluid Phase Equilibr., 149, 139-145, Doi 10.1016/S0378-3812(98)00315-X, 1998.

Good, N., Topping, D. O., Duplissy, J., Gysel, M., Meyer, N. K., Metzger, A., Turner, S. F., Baltensperger, U., Ristovski, Z., Weingartner, E., Coe, H., and McFiggans, G.: Widening the gap between measurement and modelling of secondary organic aerosol properties?, Atmos. Chem. Phys., 10, 2577-2593, 10.5194/acp-10-2577-2010, 2010.

Hallquist, M., Wenger, J. C., Baltensperger, U., Rudich, Y., Simpson, D., Claeys, M., Dommen, J., Donahue, N. M., George, C., Goldstein, A. H., Hamilton, J. F., Herrmann, H., Hoffmann, T., Iinuma, Y., Jang, M., Jenkin, M. E., Jimenez, J. L., Kiendler-Scharr, A., Maenhaut, W., McFiggans, G., Mentel, T. F., Monod, A., Prevot, A. S. H., Seinfeld, J. H., Surratt, J. D., Szmigielski, R., and Wildt, J.: The formation, properties and impact of secondary organic aerosol: current and emerging issues, Atmos. Chem. Phys., 9, 5155-5236, 2009.

Heald, C. L., Kroll, J. H., Jimenez, J. L., Docherty, K. S., DeCarlo, P. F., Aiken, A. C., Chen, Q., Martin, S. T., Farmer, D. K., and Artaxo, P.: A simplified description of the evolution of organic aerosol composition in the atmosphere, Geophys. Res. Lett., 37, -, Artn L08803, Doi 10.1029/2010gl042737, 2010.

Heaton, K. J., Dreyfus, M. A., Wang, S., and Johnston, M. V.: Oligomers in the early stage of biogenic secondary organic aerosol formation and growth, Environ. Sci. Technol., 41, 6129-6136, 10.1021/es070314n, 2007.

Hersey, S. P., Craven, J. S., Metcalf, A. R., Lin, J., Lathem, T., Suski, K. J., Cahill, J. F., Duong, H. T., Sorooshian, A., Jonsson, H. H., Shiraiwa, M., Zuend, A., Nenes, A., Prather, K. A., Flagan, R. C., and Seinfeld, J. H.: Composition and hygroscopicity of the Los Angeles Aerosol: CalNex, J. Geophys. Res.-Atmos., 118, 3016-3036, 10.1002/jgrd.50307, 2013.

Hodas, N., Zuend, A., Schilling, K., Berkemeier, T., Shiraiwa, M., Flagan, R. C., and Seinfeld, J. H.: Discontinuities in hygroscopic growth below and above water saturation for laboratory surrogates of oligomers in organic atmospheric aerosols, Atmos. Chem. Phys., 16, 12767-12792, https://doi.org/10.5194/acp-16-12767-2016, 2016.

Hosny, N. A., Fitzgerald, C., Vysniauskas, A., Athanasiadis, A., Berkemeier, T., Uygur, N., Poschl, U., Shiraiwa, M., Kalberer, M., Pope, F. D., and Kuimova, M. K.: Direct imaging of changes

in aerosol particle viscosity upon hydration and chemical aging, Chem. Sci., 7, 1357-1367, 10.1039/c5sc02959g, 2016.

Irwin, M., Good, N., Crosier, J., Choularton, T. W., and McFiggans, G.: Reconciliation of measurements of hygroscopic growth and critical supersaturation of aerosol particles in central Germany, Atmos. Chem. Phys., 10, 11737-11752, 10.5194/acp-10-11737-2010, 2010.

Irwin, M., Robinson, N., Allan, J. D., Coe, H., and McFiggans, G.: Size-resolved aerosol water uptake and cloud condensation nuclei measurements as measured above a Southeast Asian rainforest during OP3, Atmos. Chem. Phys., 11, 11157-11174, 10.5194/acp-11-11157-2011, 2011.

Jasper, J. J.: The surface tension of pure liquid compounds, J. Phys. And Chem. Ref. Data, vol 1, 841-1009, Doi: http://dx.doi.org/10.1063/1.3253106, 1972.

Jimenez, J. L., Canagaratna, M. R., Donahue, N. M., Prevot, A. S. H., Zhang, Q., Kroll, J. H., DeCarlo, P. F., Allan, J. D., Coe, H., Ng, N. L., Aiken, A. C., Docherty, K. S., Ulbrich, I. M., Grieshop, A. P., Robinson, A. L., Duplissy, J., Smith, J. D., Wilson, K. R., Lanz, V. A., Hueglin, C., Sun, Y. L., Tian, J., Laaksonen, A., Raatikainen, T., Rautiainen, J., Vaattovaara, P., Ehn, M., Kulmala, M., Tomlinson, J. M., Collins, D. R., Cubison, M. J., Dunlea, E. J., Huffman, J. A., Onasch, T. B., Alfarra, M. R., Williams, P. I., Bower, K., Kondo, Y., Schneider, J., Drewnick, F., Borrmann, S., Weimer, S., Demerjian, K., Salcedo, D., Cottrell, L., Griffin, R., Takami, A., Miyoshi, T., Hatakeyama, S., Shimono, A., Sun, J. Y., Zhang, Y. M., Dzepina, K., Kimmel, J. R., Sueper, D., Jayne, J. T., Herndon, S. C., Trimborn, A. M., Williams, L. R., Wood, E. C., Middlebrook, A. M., Kolb, C. E., Baltensperger, U., and Worsnop, D. R.: Evolution of Organic Aerosols in the Atmosphere, Science, 326, 1525-1529, Doi 10.1126/science.1180353, 2009.

Juranyi, Z., Gysel, M., Duplissy, J., Weingartner, E., Tritscher, T., Dommen, J., Henning, S., Ziese, M., Kiselev, A., Stratmann, F., George, I., and Baltensperger, U.: Influence of gas-to-particle partitioning on the hygroscopic and droplet activation behaviour of alpha-pinene secondary organic aerosol, Phys. Chem. Chem. Phys., 11, 8091-8097, Doi 10.1039/B904162a, 2009.

Kanakidou, M., Seinfeld, J. H., Pandis, S. N., Barnes, I., Dentener, F. J., Facchini, M. C., Van Dingenen, R., Ervens, B., Nenes, A., Nielsen, C. J., Swietlicki, E., Putaud, J. P., Balkanski, Y., Fuzzi, S., Horth, J., Moortgat, G. K., Winterhalter, R., Myhre, C. E. L., Tsigaridis, K., Vignati, E., Stephanou, E. G., and Wilson, J.: Organic aerosol and global climate modelling: a review, Atmos. Chem. Phys., 5, 1053-1123, 2005.

Kang, E., Root, M. J., Toohey, D. W., and Brune, W. H.: Introducing the concept of Potential Aerosol Mass (PAM), Atmos. Chem. Phys., 7, 5727-5744, 2007.

Knopf, D. A.: Thermodynamic properties and nucleation processes of upper tropospheric and lower stratospheric aerosol particles, Diss. ETH No. 15103, Zurich, Switzerland, 2003.

Krieger, U. K., Marcolli, C., and Reid, J. P.: Exploring the complexity of aerosol particle properties and processes using single particle techniques, Chem. Soc. Rev., 41, 6631-6662, 10.1039/c2cs35082c, 2012.

Kundu, S., Fisseha, R., Putman, A. L., Rahn, T. A., and Mazzoleni, L. R.: High molecular weight SOA formation during limonene ozonolysis: insights from ultrahigh-resolution FT-ICR mass spectrometry characterization, Atmos. Chem. Phys., 12, 5523-5536, 10.5194/acp-12-5523-2012, 2012.

Kuwata, M., and Martin, S. T.: Phase of atmospheric secondary organic material affects its reactivity, P. Natl. Acad. Sci. USA, 109, 17354-17359, 10.1073/pnas.1209071109, 2012.

Lambe, A. T., Chhabra, P. S., Onasch, T. B., Brune, W. H., Hunter, J. F., Kroll, J. H., Cummings, M. J., Brogan, J. F., Parmar, Y., Worsnop, D. R., Kolb, C. E., and Davidovits, P.: Effect of oxidant concentration, exposure time, and seed particles on secondary organic aerosol chemical composition and yield, Atmos. Chem. Phys., 15, 3063-3075, 10.5194/acp-15-3063-2015, 2015.

Li, Y. J., Liu, P. F., Gong, Z. H., Wang, Y., Bateman, A. P., Bergoend, C., Bertram, A. K., and Martin, S. T.: Chemical Reactivity and Liquid/Nonliquid States of Secondary Organic Material, Environ Sci Technol, 49, 13264-13274, 10.1021/acs.est.5b03392, 2015.

Liu, P. F., Abdelmalki, N., Hung, H. M., Wang, Y., Brune, W. H., and Martin, S. T.: Ultraviolet and visible complex refractive indices of secondary organic material produced by

photooxidation of the aromatic compounds toluene and m-xylene, Atmos. Chem. Phys., 15, 1435-1446, 10.5194/acp-15-1435-2015, 2015.

Liu, P. F., Li, Y. J., Wang, Y., Gilles, M. K., Zaveri, R. A., Bertram, A. K., and Martin, S. T.: Lability of secondary organic particulate matter, P. Natl. Acad. Sci. USA, 113, 12643-12648, 10.1073/pnas.1603138113, 2016.

Liu, P. F., Zhang, Y., and Martin, S. T.: Complex Refractive Indices of Thin Films of Secondary Organic Materials by Spectroscopic Ellipsometry from 220 to 1200 nm, Environ. Sci. Technol., 47, 13594-13601, Doi 10.1021/Es403411e, 2013.

Marcolli, C., and Krieger, U. K.: Phase changes during hygroscopic cycles of mixed organic/inorganic model systems of tropospheric aerosols, J. Phys. Chem. A., 110, 1881-1893, Doi 10.1021/Jp0556759, 2006.

Martin, S. T.: Phase transitions of aqueous atmospheric particles, Chem. Rev., 100, 3403-3453, Doi 10.1021/Cr990034t, 2000.

Massoli, P., Lambe, A. T., Ahern, A. T., Williams, L. R., Ehn, M., Mikkila, J., Canagaratna, M. R., Brune, W. H., Onasch, T. B., Jayne, J. T., Petaja, T., Kulmala, M., Laaksonen, A., Kolb, C. E., Davidovits, P., and Worsnop, D. R.: Relationship between aerosol oxidation level and hygroscopic properties of laboratory generated secondary organic aerosol (SOA) particles, Geophys. Res. Lett., 37, Artn L2480110.1029/2010gl045258, 2010.

O'Brien, R. E., Wang, B. B., Kelly, S. T., Lundt, N., You, Y., Bertram, A. K., Leone, S. R., Laskin, A., and Gilles, M. K.: Liquid-liquid phase separation in aerosol particles: Imaging at the nanometer scale, Environ. Sci. Technol., 49, 4995-5002, 10.1021/acs.est.5b00062, 2015.

Pajunoja, A., Lambe, A. T., Hakala, J., Rastak, N., Cummings, M. J., Brogan, J. F., Hao, L. Q., Paramonov, M., Hong, J., Prisle, N. L., Malila, J., Romakkaniemi, S., Lehtinen, K. E. J., Laaksonen, A., Kulmala, M., Massoli, P., Onasch, T. B., Donahue, N. M., Riipinen, I., Davidovits, P., Worsnop, D. R., Petaja, T., and Virtanen, A.: Adsorptive uptake of water by semisolid secondary organic aerosols, Geophys. Res. Lett., 42, 3063-3068, Doi 10.1002/2015gl063142, 2015.

Pandis, S. N., Harley, R. A., Cass, G. R., and Seinfeld, J. H.: Secondary organic aerosol formation and transport, Atmos. Environ. a-Gen, 26, 2269-2282, Doi 10.1016/0960-1686(92)90358-R, 1992.

Pankow, J. F.: Gas/particle partitioning of neutral and ionizing compounds to single and multi-phase aerosol particles. 1. Unified modeling framework, Atmos. Environ., 37, 3323-3333, Doi 10.1016/S1352-2310(03)00346-7, 2003.

Pant, A., Parsons, M. T., and Bertram, A. K.: Crystallization of aqueous ammonium sulfate particles internally mixed with soot and kaolinite: Crystallization relative humidities and nucleation rates, J. Phys. Chem. A., 110, 8701-8709, Doi 10.1021/Jp060985s, 2006.

Parsons, M. T., Mak, J., Lipetz, S. R., and Bertram, A. K.: Deliquescence of malonic, succinic, glutaric, and adipic acid particles, J. Geophys. Res.-Atmos., 109, -, Artn D06212, Doi 10.1029/2003jd004075, 2004.

Petters, M. D., Kreidenweis, S. M., Snider, J. R., Koehler, K. A., Wang, Q., Prenni, A. J., and Demott, P. J.: Cloud droplet activation of polymerized organic aerosol, Tellus B, 58, 196-205, DOI 10.1111/j.1600-0889.2006.00181.x, 2006.

Petters, M. D., and Kreidenweis, S. M.: A single parameter representation of hygroscopic growth and cloud condensation nucleus activity, Atmos. Chem. Phys., 7, 1961-1971, 2007.

Petters, M. D., Wex, H., Carrico, C. M., Hallbauer, E., Massling, A., McMeeking, G. R., Poulain, L., Wu, Z., Kreidenweis, S. M., and Stratmann, F.: Towards closing the gap between hygroscopic growth and activation for secondary organic aerosol - Part 2: Theoretical approaches, Atmos. Chem. Phys., 9, 3999-4009, 2009.

Pickering, S.: LXXI. A study of the properties of some strong solutions, J. Chem. Soc., 63, 998–1027, 1893.

Poschl, U., Martin, S. T., Sinha, B., Chen, Q., Gunthe, S. S., Huffman, J. A., Borrmann, S., Farmer, D. K., Garland, R. M., Helas, G., Jimenez, J. L., King, S. M., Manzi, A., Mikhailov, E., Pauliquevis, T., Petters, M. D., Prenni, A. J., Roldin, P., Rose, D., Schneider, J., Su, H., Zorn, S. R., Artaxo, P., and Andreae, M. O.: Rainforest aerosols as biogenic nuclei of clouds and precipitation in the Amazon, Science, 329, 1513-1516, Doi 10.1126/science.1191056, 2010.

Prenni, A. J., Petters, M. D., Kreidenweis, S. M., DeMott, P. J., and Ziemann, P. J.: Cloud droplet activation of secondary organic aerosol, J. Geophys. Res.-Atmos., 112, Artn D10223, Doi 10.1029/2006jd007963, 2007.

Prenni, A. J., Petters, M. D., Kreidenweis, S. M., Heald, C. L., Martin, S. T., Artaxo, P., Garland, R. M., Wollny, A. G., and Poschl, U.: Relative roles of biogenic emissions and Saharan dust as ice nuclei in the Amazon basin, Nat. Geosci., 2, 401-404, Doi 10.1038/Ngeo517, 2009.

Rastak, N., A. Pajunoja, J. C. Acosta Navarro, D. G. Partridge, J. Ma, M. Song, A. Kirkevåg, Y. Leong, W. W. Hu, N. F. Taylor, D. R. Collins, K. Cerully, A. Bougagioti, R. Krejci, P. Liu, T. Petäjä, C. Percival, A. M. L. Ekman, A. Nenes, S. T. Martin, J. L. Jimenez, D. O. Topping, A. K. Bertram, A. Zuend, A. Virtanen, and I. Riipinen: Microphysical explanation of the RH-dependent water-affinity of biogenic organic aerosol and its importance for climate, Geophys. Res. Lett., accepted, 2017.

Raymond, T. M., and Pandis, S. N.: Cloud activation of single-component organic aerosol particles, J. Geophys. Res.-Atmos., 107, Artn 478710.1029/2002jd002159, 2002.

Reid, J. P., Dennis-Smither, B. J., Kwamena, N. O. A., Miles, R. E. H., Hanford, K. L., and Homer, C. J.: The morphology of aerosol particles consisting of hydrophobic and hydrophilic phases: hydrocarbons, alcohols and fatty acids as the hydrophobic component, Phys. Chem. Chem. Phys., 13, 15559-15572, Doi 10.1039/C1cp21510h, 2011.

Reinhardt, A., Emmenegger, C., Gerrits, B., Panse, C., Dommen, J., Baltensperger, U., Zenobi, R., and Kalberer, M.: Ultrahigh mass resolution and accurate mass measurements as a tool to characterize oligomers in secondary organic aerosols, Anal. Chem., 79, 4074-4082, 10.1021/ac062425v, 2007.

Renbaum-Wolff, L., Song, M. J., Marcolli, C., Zhang, Y., Liu, P. F. F., Grayson, J. W., Geiger, F. M., Martin, S. T., and Bertram, A. K.: Observations and implications of liquid-liquid phase separation at high relative humidities in secondary organic material produced by alpha-pinene ozonolysis without inorganic salts, Atmos. Chem. Phys., 16, 7969-7979, 10.5194/acp-16-7969-2016, 2016.

Robinson, E. S., Saleh, R., and Donahue, N. M.: Organic aerosol mixing observed by single-particle mass spectrometry, J. Phys. Chem. A., 117, 13935-13945, 10.1021/jp405789t, 2013.

Schill, G. P., and Tolbert, M. A.: Heterogeneous ice nucleation on phase-separated organic-sulfate particles: effect of liquid vs. glassy coatings, Atmos. Chem. Phys., 13, 4681-4695, 10.5194/acp-13-4681-2013, 2013.

Shilling, J. E., Chen, Q., King, S. M., Rosenoern, T., Kroll, J. H., Worsnop, D. R., DeCarlo, P. F., Aiken, A. C., Sueper, D., Jimenez, J. L., and Martin, S. T.: Loading-dependent elemental composition of alpha-pinene SOA particles, Atmos. Chem. Phys., 9, 771-782, 2009.

Shrestha, M., Zhang, Y., Ebben, C. J., Martin, S. T., and Geiger, F. M.: Vibrational sum frequency generation spectroscopy of secondary organic material produced by condensational growth from alpha-pinene ozonolysis, J. Phys. Chem. A., 117, 8427-8436, Doi 10.1021/Jp405065d, 2013.

Smith, M. L., Bertram, A. K., and Martin, S. T.: Deliquescence, efflorescence, and phase miscibility of mixed particles of ammonium sulfate and isoprene-derived secondary organic material, Atmos. Chem. Phys., 12, 9613-9628, 10.5194/acp-12-9613-2012, 2012.

Song, M., Marcolli, C., Krieger, U. K., Zuend, A., and Peter, T.: Liquid-liquid phase separation and morphology of internally mixed dicarboxylic acids/ammonium sulfate/water particles, Atmos. Chem. Phys., 12, 2691-2712, Doi 10.5194/acp-12-2691-2012, 2012b.

Song, M., Marcolli, C., Krieger, U. K., Zuend, A., and Peter, T.: Liquid-liquid phase separation in aerosol particles: Dependence on O:C, organic functionalities, and compositional complexity, Geophys. Res. Lett., 39, Artn L19801, Doi 10.1029/2012gl052807, 2012a.

Song, M. J., Marcolli, C., Krieger, U. K., Lienhard, D. M., and Peter, T.: Morphologies of mixed organic/inorganic/aqueous aerosol droplets, Faraday Discuss., 165, 289-316, Doi 10.1039/C3fd00049d, 2013.

Song, M., Liu, P. F., Hanna, S. J., Li, Y. J., Martin, S. T., and Bertram, A. K.: Relative humidity-dependent viscosities of isoprene-derived secondary organic material and atmospheric implications for isoprene-dominant forests, Atmos. Chem. Phys., 15, 5145-5159, Doi 10.5194/acp-15-5145-2015, 2015.

Spracklen, D. V., Jimenez, J. L., Carslaw, K. S., Worsnop, D. R., Evans, M. J., Mann, G. W., Zhang, Q., Canagaratna, M. R., Allan, J., Coe, H., McFiggans, G., Rap, A., and Forster, P.: Aerosol mass spectrometer constraint on the global secondary organic aerosol budget, Atmos. Chem. Phys., 11, 12109-12136, 10.5194/acp-11-12109-2011, 2011.

Takahama, S., Schwartz, R. E., Russell, L. M., Macdonald, A. M., Sharma, S., and Leaitch, W. R.: Organic functional groups in aerosol particles from burning and non-burning forest emissions at a high-elevation mountain site, Atmos. Chem. Phys., 11, 6367-6386, Doi 10.5194/acp-11-6367-2011, 2011.

Tiryaki, A., Guruz, G., and Orbey, H.: Liquid-Liquid Equilibria of Ternary-Systems of Water Plus Acetone and C-5-Alcohol and C-8-Alcohol at 298-K, 303-K and 308-K, Fluid Phase Equilibr., 94, 267-280, Doi 10.1016/0378-3812(94)87061-6, 1994.

Veghte, D. P., Altaf, M. B., and Freedman, M. A.: Size Dependence of the Structure of Organic Aerosol, J. Am. Chem. Soc., 135, 16046-16049, 10.1021/ja408903g, 2013.

Ye, Q., Robinson, E. S., Ding, X., Ye, P. L., Sullivan, R. C., and Donahue, N. M.: Mixing of secondary organic aerosols versus relative humidity, P. Natl. Acad. Sci. USA, 113, 12649-12654, 10.1073/pnas.1604536113, 2016.

You, Y., Renbaum-Wolff, L., and Bertram, A. K.: Liquid-liquid phase separation in particles containing organics mixed with ammonium sulfate, ammonium bisulfate, ammonium nitrate or sodium chloride, Atmos. Chem. Phys., 13, 11723-11734, 10.5194/acp-13-11723-2013, 2013.

You, Y., Smith, M. L., Song, M. J., Martin, S. T., and Bertram, A. K.: Liquid-liquid phase separation in atmospherically relevant particles consisting of organic species and inorganic salts, Int. Rev. Phys. Chem., 33, 43-77, 10.1080/0144235X.2014.890786, 2014.

Zhang, Q., Jimenez, J. L., Canagaratna, M. R., Allan, J. D., Coe, H., Ulbrich, I., Alfarra, M. R., Takami, A., Middlebrook, A. M., Sun, Y. L., Dzepina, K., Dunlea, E., Docherty, K., DeCarlo, P. F., Salcedo, D., Onasch, T., Jayne, J. T., Miyoshi, T., Shimono, A., Hatakeyama, S., Takegawa, N., Kondo, Y., Schneider, J., Drewnick, F., Borrmann, S., Weimer, S., Demerjian, K., Williams, P., Bower, K., Bahreini, R., Cottrell, L., Griffin, R. J., Rautiainen, J., Sun, J. Y.,

Zhang, Y. M., and Worsnop, D. R.: Ubiquity and dominance of oxygenated species in organic aerosols in anthropogenically-influenced Northern Hemisphere midlatitudes, Geophys. Res. Lett., 34, Artn L13801, Doi 10.1029/2007gl029979, 2007.

Zhao, D. F., Buchholz, A., Kortner, B., Schlag, P., Rubach, F., Fuchs, H., Kiendler-Scharr, A., Tillmann, R., Wahner, A., Watne, A. K., Hallquist, M., Flores, J. M., Rudich, Y., Kristensen, K., Hansen, A. M. K., Glasius, M., Kourtchev, I., Kalberer, M., and Mentel, T. F.: Cloud condensation nuclei activity, droplet growth kinetics, and hygroscopicity of biogenic and anthropogenic secondary organic aerosol (SOA), Atmos. Chem. Phys., 16, 1105-1121, 10.5194/acp-16-1105-2016, 2016.

Zuend, A., Marcolli, C., Peter, T., and Seinfeld, J. H.: Computation of liquid-liquid equilibria and phase stabilities: implications for RH-dependent gas/particle partitioning of organic-inorganic aerosols, Atmos. Chem. Phys., 10, 7795-7820, Doi 10.5194/acp-10-7795-2010, 2010.

Zuend, A., and Seinfeld, J. H.: Modeling the gas-particle partitioning of secondary organic aerosol: the importance of liquid-liquid phase separation, Atmos. Chem. Phys., 12, 3857-3882, 10.5194/acp-12-3857-2012, 2012.

Table 1. Experimental conditions for production and collection of SOM particles by ozonolysis. Included is the measured separation relative humidity (SRH) upon moistening and mixing relative humidity (MRH) upon drying of the collected particles. Particles were collected on hydrophobic substrates using an electrostatic precipitator or single stage impactor. The uncertainty in the MRH and SRH values are ± 2.0 % RH, due to the uncertainty in the RH measurements.

SOM sample	VOC conc. (ppm)	O_3 conc. (ppm)	SOM mass conc. ($\mu g\ m^{-3}$)*	Flow rate for SOM particle production ($L\ m^{-1}$)	Collection time (hour)	Collection method	MRH (%)	SRH (%)
β-caryophyllene 1	0.03	30	15-30	7.0	24	Single stage impactor	92.7	94.9
β-caryophyllene 2	0.03	30	15-30	7.0	46	Single stage impactor	95.0	94.4
β-caryophyllene 3	0.7	12	2000-4000	3.5	6	Electrostatic precipitator	90.9	91.5
β-caryophyllene 4	0.7	12	2000-4000	3.5	14	Electrostatic precipitator	93.9	94.1
β-caryophyllene 5	0.7	12	2000-4000	3.5	9	Electrostatic precipitator	93.9	94.1
Limonene 1	0.07	30	80-90	7.0	24	Single stage impactor	95.6	98.7
Limonene 2	0.07	30	80-90	7.0	24	Single stage impactor	97.4	98.8
Limonene 3	2.0	13	7000	3.5	20	Electrostatic precipitator	95.6	95.3
Limonene 4	2.0	13	7000	3.5	20	Electrostatic precipitator	92.7	94.5

* Values derived from number-diameter distribution measured by an SMPS and analyzed using a material density of 1200 $kg\ m^{-3}$.

Table 2. Experimental conditions for production and collection of SOM produced by photo-oxidation. Included are the measured separation relative humidity (SRH) upon moistening and mixing relative humidity (MRH) upon drying of the collected particles. Particles were collected on hydrophobic substrates using an electrostatic precipitator or single stage impactor. SRH = 0 and MRH = 0 indicates LLPS was not observed during humidity cycles.

SOM sample	VOC conc. (ppm)	O_3 conc. (ppm)	SOM mass conc. ($\mu g\ m^{-3}$)*	Flow rate for SOM particle production ($L\ m^{-1}$)	Collection time (hour)	Collection method	MRH (%)	SRH (%)
Toluene 1	0.2	30	80-100	7.0	20	Single stage impactor	0	0
Toluene 2	0.2	30	80-100	7.0	24	Single stage impactor	0	0
Toluene 3	1.0	30	600-1000	7.0	48	Electrostatic precipitator	0	0
Toluene 4	1.0	30	600-1000	7.0	48	Electrostatic precipitator	0	0
Toluene 5	1.0	30	600-1000	7.0	96	Electrostatic precipitator	0	0
Toluene 6	1.0	30	600-1000	7.0	96	Electrostatic precipitator	0	0

* Values derived from number-diameter distribution measured by an SMPS and analyzed using a material density of 1200 kg m^{-3}.

Table 3. Summary of the LLPS results as well as the average oxygen-to-carbon atomic ratios (O:C) of the studied SOM particles. The standard deviation (σ) of the separation relative humidity (SRH) and mixing relative humidity (MRH) is derived from several cycles of RH for different SOM mass concentrations. SRH = 0 and MRH = 0 indicates phase separation was not observed. The average O:C values for SOM from toluene photo-oxidation are based on the current study (Section 2.1). The average O:C values for the other SOM are taken from the literature. Since the average O:C can depend on oxidant time and oxidation conditions, we chose literature data that were closest to the experimental conditions used in the LLPS studies (Supplementary Material, Section S1 and Table S1).

SOM	Average O:C		Average RH (%) ± σ	
	Lowest	Highest	MRH	SRH
Ozonolysis of β-caryophyllene	0.36[a]	0.38[a]	93.3 ± 1.7	93.8 ± 1.3
Ozonolysis of α-pinene	0.42[a]	0.44[a]	95.9 ± 0.8[b]	96.1 ± 0.6[b]
Ozonolysis of limonene	0.34[c]	0.40[c]	95.3 ± 1.9	96.8 ± 2.2
Photo-oxidation of isoprene	0.52[d]	0.89[a]	0[e]	0 [e]
Photo-oxidation of toluene	1.14[f]	1.30[f]	0	0

[a] Li et al. (2015); [b] Renbaum-Wolff et al. (2016); [c] Heaton et al. (2007); [d] Lambe et al. (2015); [e] Rastak et al. (2017); [f] This study.

Table 4. Literature data of measured average O:C, κ_{HGF}, κ_{CCN} , and the difference between κ_{HGF} and κ_{CCN}, denoted as $\Delta\kappa$, of SOMs. The average O:C values are based on measurements from the individual studies referenced here. The experimental conditions for the studies reported in Table 4 were not necessarily similar to the experimental conditions for the studies reported in Table 3, even if the same precursor volatile organic compound was used.

SOM	O:C	κ_{HGF} at 90% RH	κ_{CCN}	$\Delta\kappa$	Reference
Photo-oxidation of α-pinene	0.4	0.04	0.15	0.11	Massoli et al. (2010)
	0.43	0.07	0.16	0.09	Massoli et al. (2010)
	0.45	0.03	0.11	0.08	Pajunoja et al. (2015)
	0.55	0.10	0.12	0.02	Pajunoja et al. (2015)
	0.67	0.14	0.18	0.04	Massoli et al. (2010)
	0.70	0.12	0.13	0.01	Pajunoja et al. (2015)
Photo-oxidation of isoprene	0.86	0.13	0.14	0.01	Pajunoja et al. (2015)
Photo-oxidation of longifolene	0.39	0.02	0.10	0.08	Pajunoja et al. (2015)
	0.56	0.03	0.09	0.06	Pajunoja et al. (2015)
	0.83	0.08	0.10	0.02	Pajunoja et al. (2015)

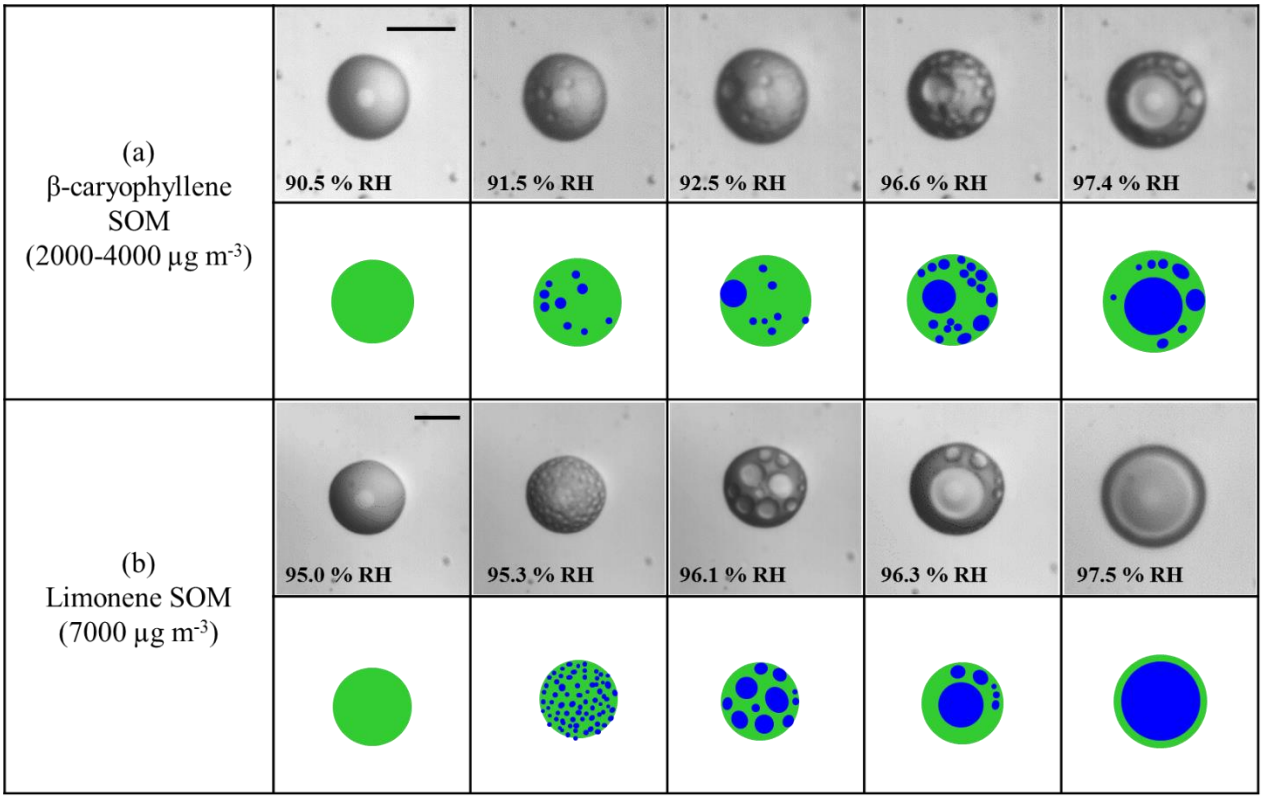

Figure 1. Optical images of SOM particles with increasing RH: (a) β-caryophyllene-derived SOM for the mass concentrations of 2000 - 4000 µg m^{-3} (β-caryophyllene 3, Table 1) and (b) limonene-derived SOM for the mass concentrations of 7000 µg m^{-3} (Limonene 3, Table 1). Note that the light gray circles at the center of the particles are an optical effect due to the hemispherical nature of the particles. Illustrations are shown below the images for clarity. Green: SOM-rich phase. Blue: water-rich phase. The scale bar is 20 µm.

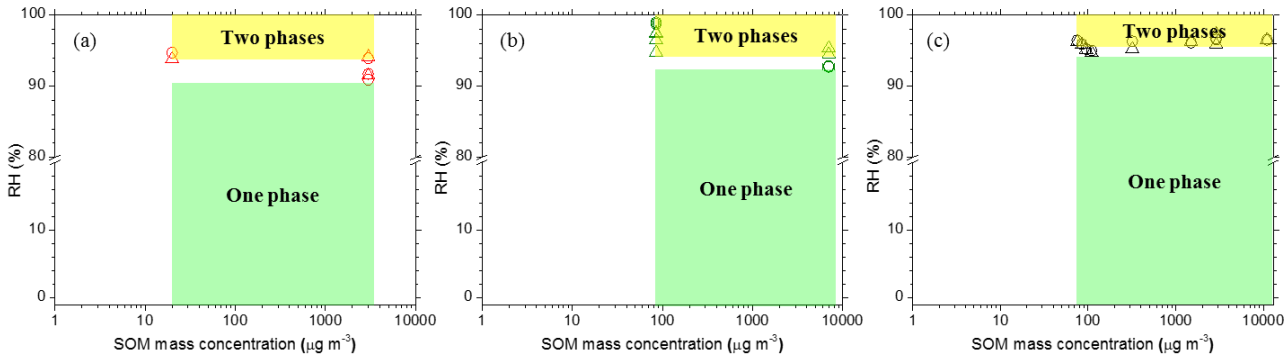

Figure 2. RH at which two phases were observed during humidity cycles of individual particles of (a) β-caryophyllene-derived SOM and (b) limonene-derived SOM from this study, and (c) α-pinene-derived SOM from Renbaum-Wolff et al. (2016) as a function of the SOM mass concentrations. For all panels, circles represent onset of phase separation upon moistening (i.e. separation relative humidity, SRH) and triangles represent mixing of two liquid phases upon drying (i.e. mixing relative humidity, MRH). Yellow shaded region indicates two phases present and green shaded region indicates one phase prevalent in SOM. SOM mass concentrations were derived from measured number-diameter distributions and assuming a material density of 1200 kg m^{-3} (Liu et al., 2013).

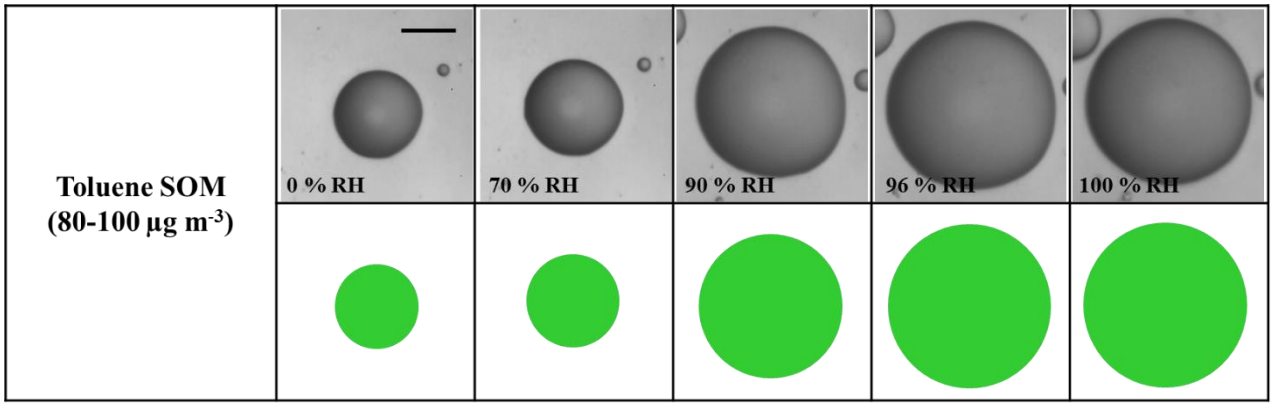

Figure 3. Optical images of toluene-derived SOM for the particle mass concentrations of 80 - 100 µg m^{-3} (Toluene 2, Table 2) with increasing RH. Illustrations of the images are shown for clarity. Green: SOM-rich phase. Size bar is 20 µm.

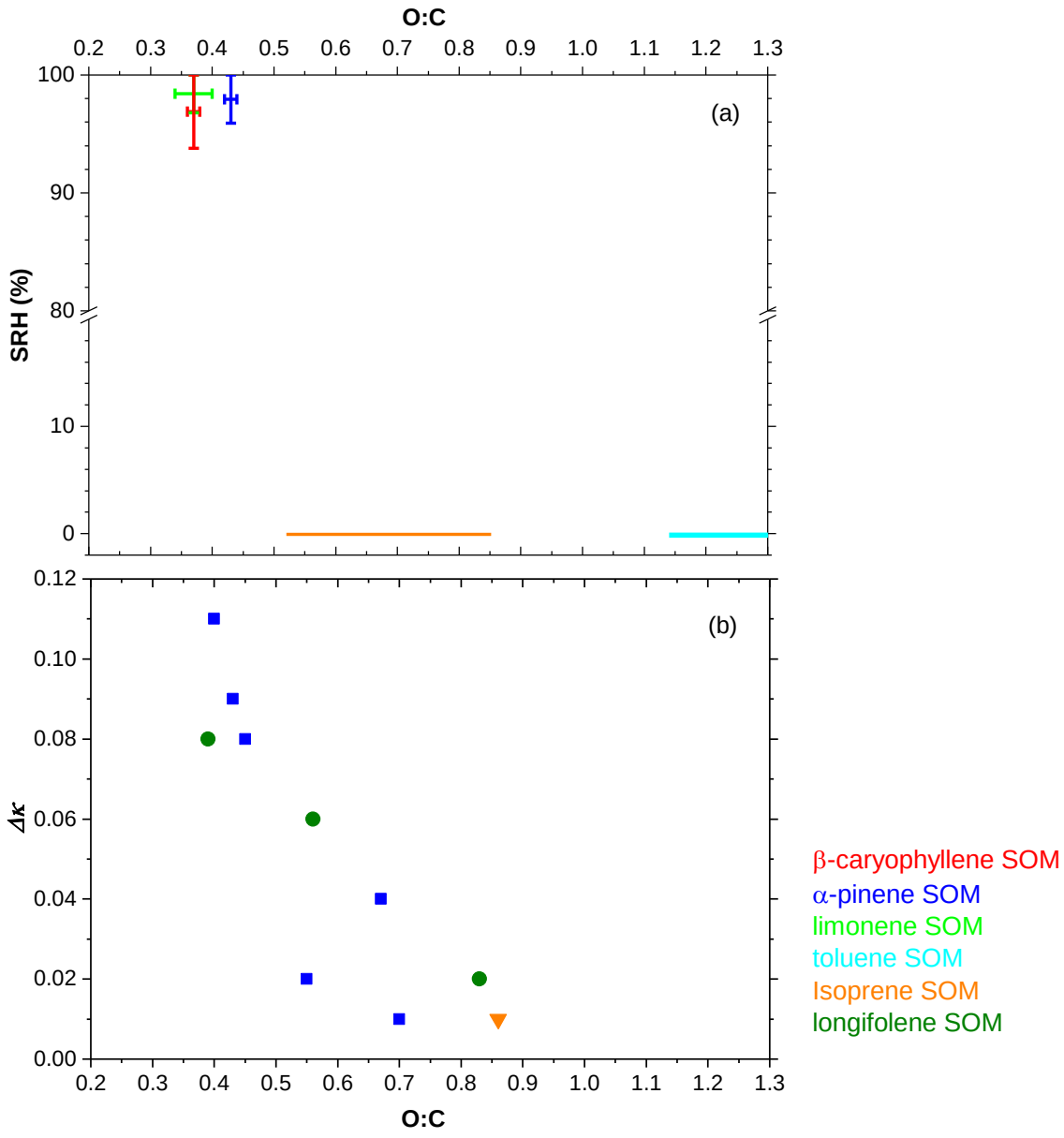

Figure 4. (a) Separation relative humidity (SRH) as a function of the average O:C of the organic material. Shown are the results from Table 3. β-caryophyllene-derived SOM (red), limonene-derived SOM (light green), and toluene-derived SOM (cyan) from this study, isoprene-derived SOM (orange) from Rastak et al. (2017) and α-pinene-derived SOM (blue) from Renbaum-Wolff et al. (2016) as a function of O:C. RH value of 0 % indicates that LLPS did not occur. The O:C values of the SOM particles were taken from Table 3. (b) The difference between κ_{HGF} and κ_{CCN},

denoted as $\Delta\kappa$, as a function of the average O:C of the SOM. Data taken from Table 4. The experimental conditions for the studies reported in Panel (a) were not necessarily similar to the experimental conditions for the studies reported in Panel (b), even if the same precursor volatile organic compound was used.